Multi-objective optimization of hybrid PEMFC/Li-ion battery propulsion systems for small and medium size ferries

*D. Pivetta, C. Dall'Armi, R. Taccani**

Department of Engineering and Architecture, University of Trieste, Via Valerio 10, 34127 Trieste, Italy

HIGHLIGHTS

- Optimal design and operation of a hybrid PEMFC/Li-ion battery propulsion system.
- Optimization-based approach to concurrently minimize costs and PEMFC degradation.
- Reduction of PEMFC degradation by up to 65% respect only cost minimization method.
- The limited PEMFC degradation implies an unavoidable increase in battery capacity.

ARTICLE INFO

Keywords:
Fuel cells degradation
Hydrogen
Ship propoulsion
Li-ion battery degradation
Gurobi optimizer
MILP approach

ABSTRACT

Hybrid Polymer Electrolyte Membrane Fuel Cells/Lithium-ion battery powertrains are a promising solution for zero-local-emissions marine propulsion. The present study aims to optimize the design and operation of such hybrid powertrain for small-size passenger ferries, taking into account the performance degradation of both fuel cells and batteries. A Mixed-Integer Linear-Programming approach and a hierarchical method are adopted to concurrently minimize the fuel cells degradation, the capital expenditure and the operating expenditure, while constraints are included in the model to limit the battery degradation. The results show that the proposed multi-objective optimization can lead to a reduction of fuel cells degradation by up to 65% compared to a cost-minimization only. However, this can imply an increase in the battery capacity by up to 136%. The proposed method has general validity, and it is a useful tool for both preliminary design and choice of the optimal energy management strategy for ships energy systems.

Introduction

With around 940 million annual tons of CO_2, the maritime transport is responsible for about 3% of global greenhouse gases emissions [1,2]. Recently, the International Maritime Organization (IMO) and other bodies imposed new rules that aim to mitigate the climate impact of the shipping sector [3]. Such regulations represent a turning point in the maritime industry, affecting the entire process of ship design. Indeed, several fuel consumption and emission reduction strategies have been identified, regarding, for example, hull resistance reduction, waste heat recovery on board, combustion improvement, and alternative fuels and/or power systems.

* *Corresponding author*.
E-mail address: taccani@units.it (R. Taccani).

Among the latter, Fuel Cells (FC) systems have seen a growing interest in the last years as they could guarantee zero emission propulsion [4]. In particular, Polymer Electrolyte Membrane FC (PEMFC) represent today the most mature technology, at least in sector other than shipping, and are considered a potentially very promising candidate for transportation (e.g. automotive sector) [5].

Notwithstanding the clear advantages of PEMFC in terms of emissions, the design and application of such systems on board of ships entails several issues and challenges. Firstly, PEMFC require high purity hydrogen (>99.995% of hydrogen in mass) entering the anode, in order to avoid poisoning of the platinum-based catalyst. If hydrogen is directly stored on board in its pure form, the space and safety issues linked to the storage system and the lack of hydrogen bunkering infrastructure are amongst the main issues that currently hamper the diffusion of such systems on a large scale [6]. Indeed, marine PEMFC still represent a niche market, even though the guidelines and draft codes available today could accelerate future applications [7,8].

As for the design of PEMFC propulsion systems, a key point is represented by the FC operation in dynamic load conditions. In fact, while FC have good capability to follow the power demand during steady state operation, rapid load variations would stress the FC membrane, resulting in an increase FC degradation [9,10]. Moreover, due to the relatively high cost of FC compared to traditional Internal Combustion Engines (ICE), it is opportune to hybridize FC systems with an Energy Storage System (ESS) to meet the total power demand, avoiding large FC installed power. Among different types of ESS, lithium-ion (Li-ion) batteries cover, today, the largest market share in the transport sector thanks to their higher energy density compared to other commercial secondary batteries, and have already been implemented also in shipping applications [11,12].

The ratio of FC power to the total power demand depends on the role of the ESS, but generally the FC should provide the base load, while the ESS covers the peak transients [13]. In this context, the comprehensive review by Pollet et al. [14] on the current status of FC Hybrid Vehicles (FCHV) points out that hybrid powertrains involve lower FC installed power and hence lower costs. In addition, it is stated that an appropriate control strategy of FCHV could avoid the peak operation of both FC and batteries, improving the components lifetime.

The study of load allocations and of the Energy Management Strategy (EMS) can lead to an overall improvement of the energy plant operation (in terms of energy efficiency, cost, etc.). This aspect has been widely investigated for the application of hybrid powertrains in the automotive sector and starts to be examined also in the maritime industry. Two different approaches can be followed for the definition of EMS: rule-based and optimization-based. The first approach defines the EMS on the basis of rules delineated from the human expertise in the field. Optimization-based approach, instead, outlines the best EMS through the optimization of the energy system (e.g. pursuing technical, economic, environmental, or social targets). Optimization can be either global (i.e. on the overall operation profile) or real time. The latter implies high computational effort but has been widely used especially in the automotive sector since the optimization can be performed even if the driving cycle is not known in advance. Extensive reviews on both rule-based and optimization-based EMS are reported in Refs. [15,16] with reference to automotive applications. In particular, Yue et al. [16] analyze the possibility to define health-conscious EMSs that account for both FC and Li-ion battery degradation during the system operation. The review concludes that the future trend would be the development of multi-objective optimization problems that take into account the degradation of the energy units, with a special focus on achieving a good balance between complexity and optimality of the system.

The aforementioned studies refer to FCHV, but the information has general validity and can be transposed to the maritime sector. Indeed, research and applications of hybrid FC/ESS propulsion systems in the shipping industry are still limited compared to the automotive ones, even though several studies can be found in the literature.

An extensive overview of hybrid ship propulsion systems is presented by Geertsma et al. [17], where both mechanical and electrical propulsion hybrid systems are reviewed. As of the electrical propulsion systems, the hybridization with an ESS is analyzed for different main power suppliers (e.g. ICE, gas turbines, FC, batteries). The paper shows that the benefits of the ESS in a hybrid power system could be diverse, for example the possibility to switch off one of the main engines when they would run inefficiently, the opportunity for peak shaving and load levelling, the reduction of fuel consumption and local emissions, or the provision of back-up power during a failure.

Other studies available in the literature [18–25] specifically address FC/ESS hybrid systems. For example, Choi et al. [18] study the development and demonstration of a PEMFC/ESS hybrid propulsion system for a 20 m long tourist boat in Korea. The PEMFC installed power and battery capacity are respectively 50 kW and 47 kWh, where PEMFC cover the base load and battery is used for peak shaving. Taccani et al. [19] analyze the technical feasibility of the installation of a hybrid PEMFC/Li-ion battery energy system for the propulsion of a small passenger ferry fuelled by hydrogen. The rule-based EMS encompasses PEMFC for covering the average load and batteries for peak shaving. Rivarolo et al. [20,21] propose a general approach for the analysis of a PEMFC system on board of ships in terms of energy efficiency, CO_2 emissions, and costs. In particular, in Ref. [21] different power generation configurations (i.e. micro gas turbines, PEMFC, solid oxide FC) are analyzed in order to find the best EMS of a cruise ship. A genetic algorithm is used to minimize the annual variable cost of the plant. In Refs. [13,22,23] different rule-based EMS are applied to FC/ESS hybrid ferries. In all cases, rules are defined on the basis of batteries State Of Charge (SOC) and the ferry power demand. Other rule-based EMS are proposed in Ref. [24], where Su et al. propose a general methodology for the secure and stable operation of hybrid FC/ESS ship power systems. Wu et al. [25] eventually develop an EMS for the optimization of a plug-in hybrid PEMFC/Li-ion battery coastal ferry. The study aims to determine the size of FC and battery that concurrently minimize the average voyage cost and the Global Warming Potential (GWP) emissions of a vessel single voyage. It is assumed that the batteries can only be charged at ports with onshore power. FC degradation rate is calculated as function of the operating conditions, while for batteries it is assumed an average degradation rate at each time step calculated on the basis of specific lifetime. More in detail, Wu et al. [25] evaluate the FC performance degradation as proposed by Chen et al. [26]. More in detail, the reduction of a single cell voltage at the same current values. The single cell degradation describes the ageing process of the entire PEMFC stack subject to load variation, power supplied, and start/stop cycles. The results report a minimum 65% GWP emission reduction, however no data on the FC performance degradation over one-voyage are reported.

Similar approaches for evaluating PEMFC degradation have been used by Fletcher et al. [27], and Balestra et al. [28]. As for Li-ion batteries degradation, Refs. [29,30] describe the battery performance degradation as function of temperature, SOC and C-rate. In order to avoid excessive computational efforts implied by this approach, alternative methods have been developed. In particular, in Refs. [31,32] the Li-ion battery degradation is included as a constraint in the analysis of energy systems.

In this context, the present paper aims to find the best Design and Operation (D&O) of a hybrid PEMFC/Li-ion batteries energy system for the propulsion of Ro-Pax ferries, taking into account the performance degradation of both FC and batteries. More in detail, a multi-objective optimization model has been set to concurrently minimize the FC degradation and the daily cost (CAPEX and OPEX) of the vessels, while the battery degradation constrains the minimum battery capacity to be installed on board. This modeling approach represents an innovative method for the D&O optimization of marine propulsion systems.

The analyses have been performed on three different Ro-Pax ferries (small to medium size), characterized by short and frequent coastal routes during the day, as this type of ships could be particularly suitable for advantageous application of hybrid FC/ESS powertrains. It is assumed to have only one hydrogen refueling per day and that the batteries cannot be charged with onshore power. These choices have been made in order to limit as much as possible the overall complexity of the ground infrastructure (e.g. plug-in infrastructure, refueling stations). In addition, hydrogen could be produced by exploiting the availability of energy from renewable sources and then stored without a relevant self-discharge rates, as reported in several recent studies [33–38].

Among different approaches proposed in the literature for the optimization of ship energy systems (see e.g. Refs. [39–42]), a Mixed-Integer Linear Programming (MILP) approach has been chosen in this study. This method has been widely applied in similar studies available in the literature for both ships and on-land applications (e.g. Refs. [43–46]), where different production units jointly operate for the satisfaction of a time variable power demand. An extensive synthesis of MILP approach is proposed by Rech in Ref. [47], where the author reports a detailed description on variables, equations, operational constraints and objective functions that are required for the dynamic optimization of such systems.

The first part of the paper describes the energy systems considered and the main characteristics of the ferries analyzed in the case studies. Afterwards, the D&O optimization model is described and results are presented and discussed.

Case study

This study aims to analyze the optimal design and operation of Ro-Pax ferry energy systems, based on PEMFC, fuelled by hydrogen, stored in cryogenic form. As for ESS, Li-ion batteries with Nickel Manganese Cobalt Oxide chemistry (NMC) have been chosen given their high specific energy and their maturity for maritime applications [11].

Three Ro-Pax ferries are chosen to compare the optimization results, i.e. the optimal D&O variables of hybrid FC/battery system. Ferries are different in terms of size, power installed onboard, and typical operative profile (see Table 1 for the technical characteristic). Existing power generation systems are taken as reference for volume and weight available for the installation of the new energy systems.

Fig. 1 shows the power demand profiles of the three ferries, used as input data of the optimization problem. For each ferry, power demand at each time step is evaluated as function of typical speed data available on [48]. Cubic polynomial fits are used to approximate the speed-power relationship of each vessel, as proposed for example in Ref. [49]. Auxiliaries power demand are estimated in accordance with typical values for each ferry. Each electrical demand is evaluated for 1-min intervals. At each time step, the energy system (presented in Section) shall fulfil the entire energy demand of the ferries.

Energy system description

This section aims to describe the energy system proposed to fulfil electricity demand of ferries. Fig. 2 shows the conceptual schematic of a ferry energy system, where design parameters variables are written in red and operation variables in green. The first ones identify the size of the energy conversion and storage units that are chosen according to the EMS optimization criteria. The second ones are input and output power flows.

As shown in Fig. 2, cryogenic storage has been adopted for hydrogen at a temperature of 20 K and pressure of about 1 bar. Liquid hydrogen can reach an energy density of about 70 g/l, and hence could be an interesting alternative for maritime FC applications in terms of volume and weight of the storage system. Nevertheless, the use of liquefied hydrogen storage on board entails severe safety implications, even if some barriers

Table 1 – Main technical characteristics of the considered ferries.

	Very small ferry	Small ferry	Medium ferry
Length x Width (m)	42.0 × 9.4	57.9 × 13.1	88.6 × 13.6
Gross tonnage (tons)	282	630	2,055
Propulsion engine (kW)	2 × 206	2 × 637	2 × 746
Auxiliary engine (kW)	2 × 28	2 × 200	534
Engine volume (m^3)	15.5	44.9	56.2
Engine weight (kg)	7,185	20,928	26,160

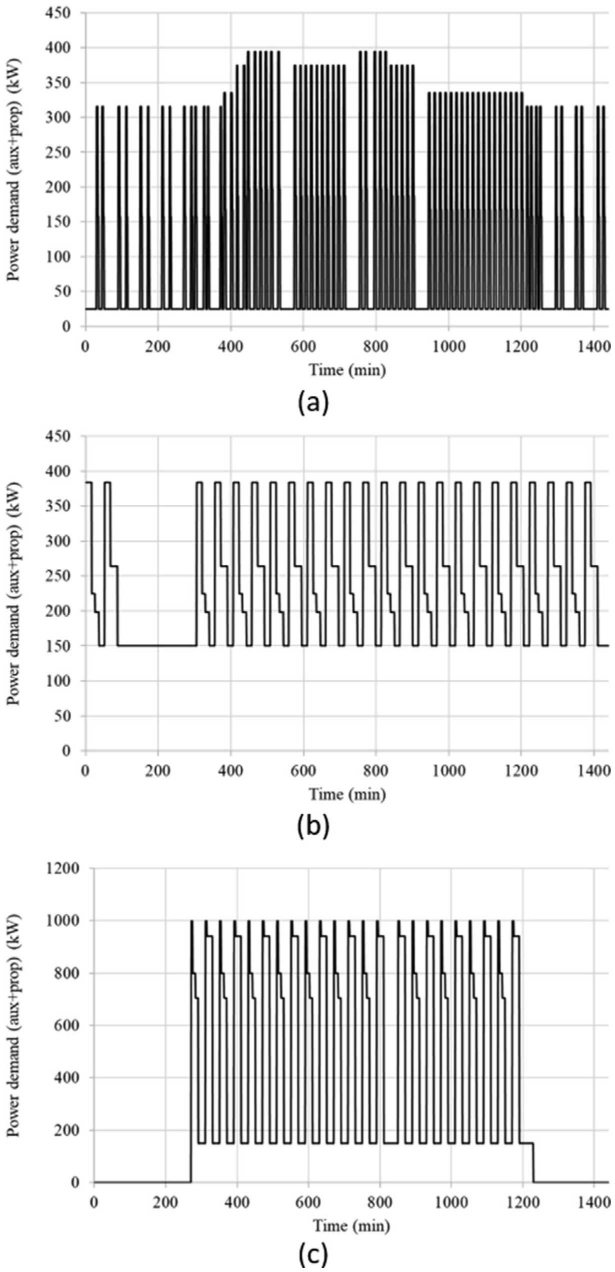

Fig. 1 — One-day power demand profile of: very small-size ferry (a), small-size ferry (b) and medium-size ferry (c).

of using cryogenic gases for ship propulsion have been overcome as today liquefied natural gas is already a logistic fuel in marine applications and IMO has published the "International Code of Safety for ships using gases or other low flash point fuels" (IGF Code [7]) [50–55]. In the proposed energy system, the stored liquefied hydrogen is pumped to a vaporizer, indirectly heated by seawater or air. After that, gaseous hydrogen at a pressure between 5 and 30 bar passes through a reduction valve to power PEMFC. This type of fuel cell requires hydrogen at a temperature of about 20 °C–60 °C and pressure of about 1 bar–1.5 bar. The energy demand of the fuel management system is considered constant at varying load. In the same way, global electric efficiency of the power conditioning system is assumed to be constant and equal to 95%.

Methods

This section aims to present the simulation model implemented to optimize the design and operation of the proposed energy system. The behavior of conversion and storage units, i.e. PEMFC stacks and Li-ion battery, is described using mathematical relations, shown in Eqs. (4)–(19). An innovative approach allows to include the performance degradation model for both FC and battery in the D&O optimization. In this way, energy system operation depends on the optimal operation of the single units, in terms of energy performance and degradation.

Characteristics of the optimization model are outlined with specific emphasis on the choice of the objective functions and on the characteristics of the equations included in the model of each conversion or storage units. A MILP approach is chosen, since the performance characteristic curves of the units can be linearized without a significant loss in accuracy, while obtaining a lower computational effort than other approaches [44,46,47]. Binary variables (δ in Eqs. (1)–(14)) are used to decide about activation/de-activation of each unit during operation. A flow-chart of the optimization approach is shown in Fig. 3.

The optimization model is written with Python programming language [56] and solved with Gurobi Optimizer [57].

The MILP optimization problem is set as:

Find $\mathbf{x}^*(t)$ and $\boldsymbol{\delta}^*(t)$ (i.e. the optimum values of the continuous, $\mathbf{x}$, and binary, $\boldsymbol{\delta}$, decision variables associated with the design and operation of the energy system) that maximize or minimize the objective function Z (Eq. (1)) subject to the constraint equations $\mathbf{g}(t)$ and inequalities $\mathbf{h}(t)$ (Eqs. (2) and (3)), on which the model of the energy system of the considered ships is based.

$$Z = f(\mathbf{x}^*(t),\ \boldsymbol{\delta}^*(t)) \tag{1}$$

$$\mathbf{g}(\mathbf{x}^*(t),\ \boldsymbol{\delta}^*(t)) = 0 \tag{2}$$

$$\mathbf{h}(\mathbf{x}^*(t),\ \boldsymbol{\delta}^*(t)) \leq 0 \tag{3}$$

The following subsections shows the g(t) and h(t) relationships in Eqs. (2) and (3) and the Z objective functions in Eq. (1), and the method used to optimize multi-objective function systems.

PEMFC stacks model

The design decisional variable of PEMFC is n, defined as the optimal number of FC stacks included in the energy system. With this modeling approach, the D&O optimization model has a limited computational effort, and it is possible to use linear curves to approximate with a good accuracy the characteristic curves of FC. Usually PEMFC are modularized and manufacturers propose fixed stacks size. According to these assumptions, it is considered that a single stack has a nominal electric power of 100 kW ($P_{FC_{max}}$). A typical performance

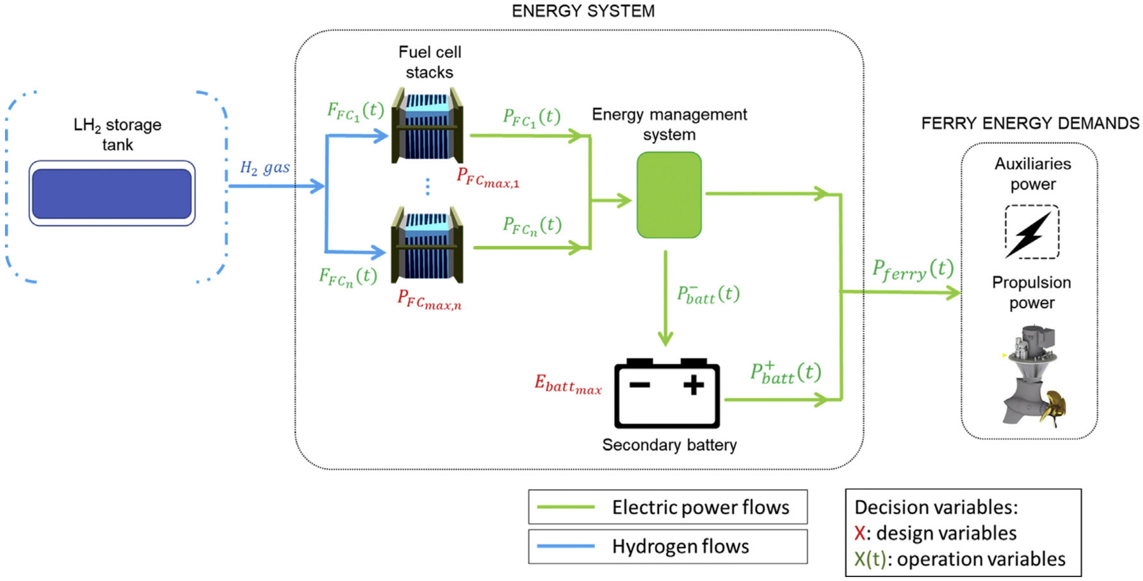

Fig. 2 – Energy system conceptual schematic. Design variables: FC stack nominal power ($P_{FC_{max,i}}$), battery energy capacity ($E_{batt_{max}}$). Operation variables: FC stack input power ($F_{FC_i}(t)$), FC stack output power ($P_{FC_i}(t)$), battery input power ($P^-_{batt}(t)$), battery output power ($P^+_{batt}(t)$), ferry power demand ($P_{ferry}(t)$).

characteristic curve, i.e. FC efficiency at varying FC power load, has been elaborated on the basis of commercial products for marine applications [58–61]. In order to simplify the overall mathematical structure of the optimization problem, it has been decided to represent the FC characteristic curve in terms of fuel consumption per power output. The fuel consumption has been expressed in kW, and is defined as the ratio between the FC power output and the FC efficiency.

Fig. 4 shows the characteristic curve of a 100 kW PEMFC stack; the y-axis identifies the fuel consumption per hour (measured in kW), the x-axis the electric power produced by the stack. It can be noted that the curve is well approximated with a linear curve in the PEMFC stack operation range (from 20% to 100% of the nominal power). Other nominal power values for the stacks could be easily implemented in the model by modifying the characteristic curves of the proposed ones.

Equations describing i-th PEMFC stack operation are:

$$F_{FC_i}(t) = k_{1FC} * P_{FC_i}(t) + k_{2FC} * \delta_{FC_i}(t) + \delta_{st,up_i}(t) * F_{start} * P_{FC_{max}} \quad (4)$$

$$k_{FC,min} * P_{FC_{max}} * \delta_{FCi}(t) \le P_{FC_i}(t) \le k_{FC,\,max} * P_{FC_{max}} * \delta_{FC_i}(t) \quad (5)$$

$$\Delta_{P_{FC}} \ge |P_{FC_i}(t) - P_{FC_i}(t-1)| \quad (6)$$

$$0 \le \delta_{FC_i}(t) - \delta_{FC_i}(t+1) + \delta_{st,up_i}(t) \quad (7)$$

where:

- k_{1FC} and k_{2FC}=linearization coefficients of the stack operation;
- $P_{FC_i}(t)$=power output of PEMFC i-th stack (in kW);
- $\delta_{FC_i}(t)$=on/off status of the i-th stack;
- $\delta_{st,up_i}(t)$=start-up phase for the i-th stack;
- F_{start}=fuel consumption in start-up phase;
- $P_{FC_{max}}$=nominal power of the i-th stack;
- $k_{FC,min}$ and $k_{FC,max}$=limits of the power i-th stack range;
- $\Delta_{P_{FC}}$=load variation allowed for the i-th stack.

Performance degradation model of PEMFC

Eqs. (8)–(12) describe the performance degradation of PEMFC stacks, which is defined as the voltage reduction of a single cell at equal current output, assuming that the behavior of a single cell can approximate the one of the entire FC stack [25–28]. The loss of power depends on:

- load variation (in Eq. (8)), defined as the variation of power (kW) between t and t+1;
- start/stop cycles (in Eq. (9)), defined as the number of start-up phases occurred for the i-th PEMFC stack, i.e. $\sum(\delta_{st,up_i}(t))$ (defined in Eq. (7));
- power converted by the *i-th* PEMFC stack (in Eq. (10)), defined in dependence of the stack current (in Eq. (11)).

For each time interval t, Eq. (12) defines the total loss of voltage for the i-th single cell, described with MILP equations.

$$dV_{load_i}(t+1) = |P_{FC_i}(t) - P_{FC_i}(t+1)| * \Delta v_{load} \quad (8)$$

$$dV_{st,up_i}(t) = \delta_{st,up_i}(t) * \Delta v_{st,up} \quad (9)$$

$$dV_{P_{FC_i}}(t) = k_{1_{dv}} * I_{FC_i}(t) + k_{2_{dv}} \quad (10)$$

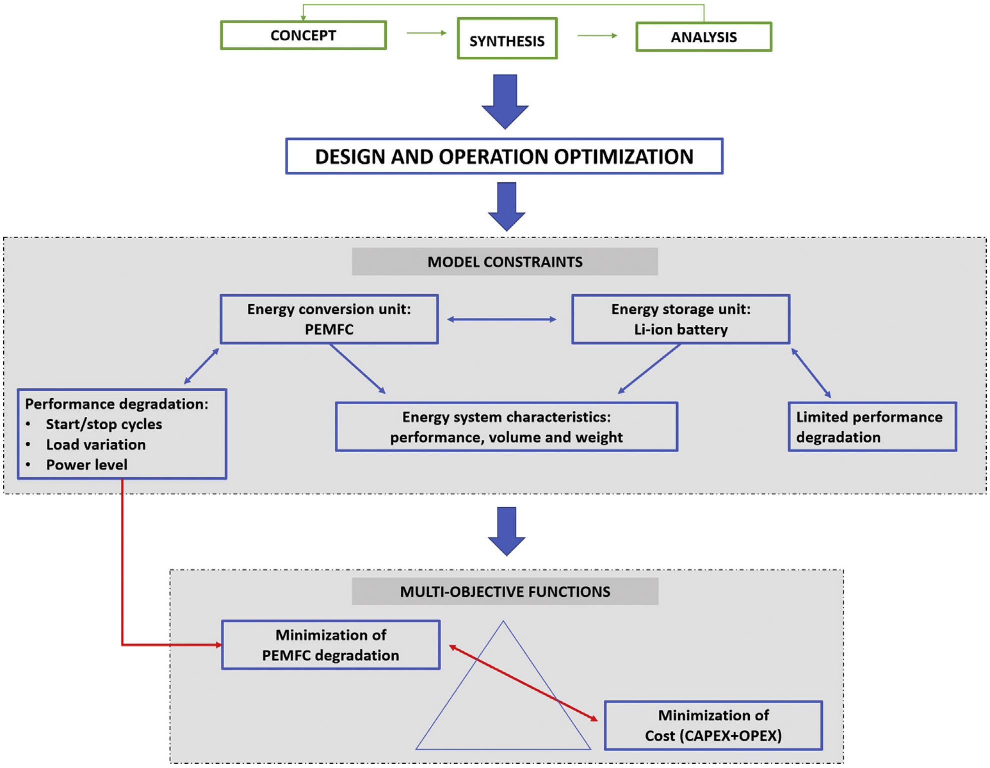

Fig. 3 – Flow-chart of the synthesis/design/operation optimization approach.

$$I_{FC_i}(t) = k_{1_I} * P_{FC_i}(t) + k_{2_I} * \delta_{FC_i}(t) \quad (11)$$

$$dV_i(t) = dV_{load_i}(t) + dV_{st,up_i}(t) + dV_{P_{FC_i}}(t) \quad (12)$$

where:

- $dV_{load_i}(t)$=voltage reduction due to load variation of i-th single cell;
- Δv_{load}=proportionality constant for load variation;
- $dV_{st,up_i}(t)$=voltage reduction due to start-up of i-th cell;
- $\Delta v_{st,up}$=constant value of voltage reduction due to start-up of i-th cell;
- $dV_{P_{FC_i}}(t)$=voltage reduction depending on the power produced by i-th cell at time t;
- $I_{FC_i}(t)$=mean current intensity supplied by the i-th cell;
- $k_{1_{dV}}$ and $k_{2_{dV}}$=proportionality constants describing voltage at varying current of i-th cell;
- k_{1_I} and k_{2_I}=proportionality constants describing current at varying power of the i-th cell;
- $dV_i(t)$=total loss of voltage in the i-th cell.

Lithium-ion battery model

The Li-ion battery operation is described by the following equations:

$$E_{batt}(t) = E_{batt}(t-1) + \left(\eta_{batt} * P^{-}_{batt}(t) - (1/\eta_{batt}) * P^{+}_{batt}(t)\right) \quad (13)$$

$$SOC_{min} * E_{battery_{max}} \leq E_{batt}(t) \leq SOC_{max} * E_{battery_{max}} \quad (14)$$

$$E_{batt}(0) = E_{batt}(t_{fin}) \quad (15)$$

where:

- $E_{batt}(t)$=energy stored in the battery at time t;
- η_{batt}=charging/discharging energy efficiency;
- $P^{+}_{batt}(t)$ and $P^{-}_{batt}(t)$=output/input battery power, respectively;
- $E_{battery_{max}}$=electrical energy capacity of the battery;
- SOC_{min} and SOC_{max}=coefficients refer to the minimum and maximum battery SOC.

The design decisional variable of Li-ion battery is the nominal energy capacity ($E_{battery_{max}}$), which is limited by the maximum and minimum SOC.

It is required that the SOC at the initial and at the final time step of the optimization period (i.e. one-day) are the same.

η_{batt} is supposed to be constant at varying of the C-rate. Given the high complexity of the energy system and the limited variation of η_{batt}, this assumption does not lead to a relevant error in the results of the optimization problem.

Performance degradation of Li-ion battery

Li-ion battery degradation can heavily affect the overall economic feasibility, the weight, and the volume of an energy plant. In this study, the Li-ion battery degradation is included in the model in a simplified way, following the procedure proposed in Refs. [31,32], in order to avoid an excessive

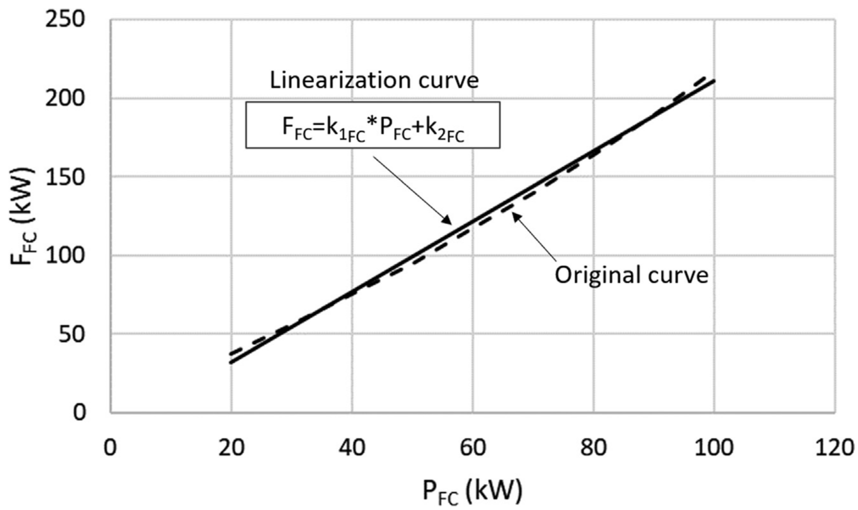

Fig. 4 – Fuel consumption at varying of the power converted by the PEMFC stack [57–60].

increase in the computational effort required for the optimization. In fact, an exhaustive model would require the use of quadratic constraints to accurately describe the behavior of Li-ion battery at varying charging/discharging electrical parameters.

Firstly, the battery capacity $E_{battery_{max}}$ is oversized to ensure the required energy storage at end of life of the battery:

$$C_{batt;os} = \frac{E_{battery_{max}}}{EoL} \tag{16}$$

where:

- $C_{batt;os}$=oversized battery capacity at end of the battery lifetime;
- $E_{battery_{max}}$=required battery capacity at the beginning of the battery lifetime;
- EoL =share of battery capacity at the end of its lifetime.

Note that the battery oversizing due to the discharge efficiency and Depth Of Discharge (DOD) is already accounted in Eqs. (13) and (14). Afterwards, assuming that the battery degrades linearly over its lifetime, an averaged battery capacity $C_{batt;av}$ is calculated as:

$$C_{batt;av} = \frac{EoL+1}{2} C_{batt;os} \tag{17}$$

A constraint is therefore included in the optimization model, defined as follows:

$$LT_{batt} * \sum_{t=t_0}^{t_{fin}} P^{+}_{batt}(t) \leq E_{tp} \tag{18}$$

where:

- LT_{batt}=battery lifetime;
- t_0 and t_{fin}=initial and final time step in the day;
- $P^{+}_{batt}(t)$=battery power supply at the time step t;
- E_{tp}=energy throughput of the battery (in kWh).

The energy throughput of the battery E_{tp} is the total amount of energy that a battery can store and deliver over its lifetime, and it is calculated as follows:

$$E_{tp} = \eta_{batt} * N_{cycle,max} * C_{batt,av} * DOD \tag{19}$$

where:

- LT_{batt}=battery lifetime;
- $N_{cycle,max}$=maximum number of battery cycles;
- DOD=Depth Of Discharge.

Energy system constraints

This section explains the relations used to describe the overall characteristics of the energy system proposed for the ferries.

Electric energy balance

The energy balance in Eq. (20) ensures that the energy system (hybrid PEMFC/Li-ion battery propulsion system) totally fulfill the ferry energy demand in each time interval t (of 1 min, i.e. $\Delta t = 1$ min). For simplicity, the equation is expressed in terms of power, being the length of the time intervals (Δt) constant.

$$\sum_{i=1}^{n} P_{FC_i}(t) + P^{+}_{batt}(t) = P_{aux}(t) + P_{prop}(t) + P^{-}_{batt}(t) \tag{20}$$

where:

- $P_{FC_i}(t)$=power supply by the PEMFC i-th stack (kW);
- $P^{+}_{batt}(t)$ e $P^{-}_{batt}(t)$=output/input battery power, respectively;
- $P_{aux}(t)$=auxiliaries power demand;
- $P_{prop}(t)$=propulsion power demand.

Volume and weight of the plant

Volume and weight are extremely important parameters for the design of ship energy systems. For this reason, Eqs. (21) and (22) limit the volume and weight of the alternative energy system within those of the conventional propulsion

Table 2 – Input parameters of the optimization model.

Parameters	Unit	Value	Ref.
c_{H_2}	€/kWh	0.3	[44]
c_{batt}	€/(kWh·day)	0.747	[11,12,31,32]
c_{FC}	€/(kW·day)	5.137	[57–60]
c_{ov}	\	0.2	N.A.
Δv_{load}	μV/ΔkW	0.0441	[25–28]
$\Delta v_{st,up}$	μV/cycle	23.91	[25–28]
DoD	%	80	[11,12,31,32]
EoL	%	80	[11,12,31,32]
η_{batt}	%	90	[11,12,31,32]
F_{start}	h	0.1	[25–28]
$k_{1_{dv}}$	μV/A	0.0351	[25–28]
$k_{2_{dv}}$	μV	0.75	[25–28]
$k_{1_{FC}}$	\	2.262	[58–61]
$k_{2_{FC}}$	kW	−14.771	[58–61]
k_{1_I}	A/kW	4.3479	[25–28]
k_{2_I}	A	−39.729	[25–28]
LT_{batt}	years	3	[12,14]
$N_{cycle,max}$	cycle	6529	[11,12,31,32]
$P_{FC_{max}}$	kW	100	N.A.
V_{batt}	m^3/kWh	0.0091	[11,12,31,32]
V_{FC}	m^3/kW	0.0312	[58–61]
V_{H_2}	m^3/kgH_2	0.17	[62–64]
w_{batt}	kg/kWh	7.98	[11,12,31,32]
w_{FC}	kg/kW	20	[58–61]
w_{H_2}	kg/kgH_2	28.5	[62–64]

systems (engine volume and weight in Table 1) increased by an acceptable correction factor to take into account the current limited development state of FC systems.

$$\sum_{i=1}^{n}\left(\int_{0}^{t_{fin}}\left(F_{FC_i}(t)*dt\right)*w_{H_2}\right)+E_{battery_{max}}*w_{batt}+n*P_{FC_{max}}*w_{FC} \leq Weight_{eng}*(1+c_{ov}) \tag{21}$$

$$\sum_{i=1}^{n}\left(\int_{0}^{t_{fin}}\left(F_{FC_i}(t)*dt\right)*V_{H_2}\right)+E_{battery_{max}}*V_{batt}+n*P_{FC_{max}}*V_{FC} \leq Volume_{eng}*(1+c_{ov}) \tag{22}$$

where:

- n=number of PEMFC stacks with an output nominal power of $P_{FC_{max}}$;
- V_{H_2}=volume occupied by hydrogen and its storage system (evaluated per energy unit, i.e. m^3/kWh);
- V_{batt}=volume occupied by the battery (evaluated per energy unit, i.e. m^3/kWh);
- V_{FC}=volume occupied by a PEMFC stack (evaluated per power unit, i.e. m^3/kW);
- w_{H_2}=weight of bunkered hydrogen and its storage system (evaluated per energy unit, i.e. kg/kWh);
- w_{batt}=weight of the battery (evaluated per energy unit, i.e. kg/kWh);
- w_{FC}=weight of a PEMFC stack (evaluated per power unit, i.e. kg/kW);
- c_{ov}=correction oversizing factor.

Objective functions

A multi-objective optimization has been used to find the best D&O of the hybrid FC/battery propulsion system, using the MILP solver Gurobi Optimizer [57]. For multi-objective optimizations a "Hierarchical Objectives" method is adopted, fixing different priorities for the objective functions. The method consists in a chain of consecutive optimizations starting from the objective function with higher priority. Among the set of solutions, which maximize/minimize the higher-priority objective function, algorithm searches for the best solutions to optimize the following objective functions in

Table 3 – Main results of the multi-objective D&O optimization (cost minimization and FC degradation minimization).

	Design				Operation		
	FC nominal power (kW)	Battery installed capacity (kWh)	Volume of main units (m^3)	Weight of main units (ton)	Daily cost (€/day)	FC degradation (μV/day)	H_2 consumption (kg/day)
Very small-size ferry	2 × 100	286	8.3	6.2	2590	214.5	157
Small-size ferry	4 × 100	330	14.9	11.0	5335	212.6	351
Medium-size ferry	6 × 100	657	23.5	17.5	8074	230.5	519

Table 4 – Main results of the single-objective D&O optimization (only cost minimization).

	Design				Operation		
	FC nominal power (kW)	Battery installed capacity (kWh)	Volume of main units (m^3)	Weight of main units (ton)	Daily cost (€/day)	FC degradation (μV/day)	H^2 consumption (kg/day)
Very small- size ferry	2 × 100	202	7.7	5.7	2456	620.5	152
Small-size ferry	3 × 100	140	10.4	7.8	4893	565.4	359
Medium-size ferry	7 × 100	377	24.6	17.7	7927	366.8	497

priority order. The optimum solution is chosen among the solutions that do not worsen the previous objective functions, unless a gap from the best values of the previous objective functions is allowed (see Ref. [57]).

In this work, two objective functions have been specified, namely cost (f_1 in Eq. (23)) and FC degradation (f_2 in Eq. (24)). The first function describes the cost of one-day operation of the energy system, taking into account the CAPEX and OPEX of energy units, the second one describes the performance degradation of the PEMFC stacks included in the energy systems. In this case, a higher priority has been set for the minimization of f_2 and a 10% deviation from the optimal value of the function is allowed.

$$f_1 = \sum_{i=1}^{n}\left(\int_0^{t_{fin}} \left(F_{FC_i}(t) * dt\right) * c_{H_2}\right) + E_{battery_{max}} * c_{batt} + n * P_{FC_{max}} * c_{FC} \tag{23}$$

$$f_2 = \sum_{i=1}^{n}\left(\int_0^{t_{fin}} dV_i(t)\right) \tag{24}$$

where:

- c_{H_2}=hydrogen cost (evaluated per energy unit, i.e. €/kWh);
- c_{batt}=battery cost (evaluated per energy unit, i.e. €/kWh);
- c_{FC}=PEMFC stack cost (evaluated per power unit, i.e. €/kW).

The results of the multi-objective optimization are then compared with the ones of a single-objective optimization for cost minimization (f_1 in Eq. (23)). In this way, it is possible to appreciate the influence of the objective function f_2 (Eq. (24)) in the overall optimization of the system. In Tables 3 and 4, the optimal values of the objective functions f_1 and f_2 are reported in "Daily cost" and "FC degradation" columns, respectively.

Results

In this section, the optimization results are presented and discussed for each of the three vessels. More in detail, Table 2 reports the parameters adopted in the optimization. The parameters referring to PEMFC and battery are calculated according to data collected from the literature and elaborated on the basis of commercial devices. As for PEMFC and battery CAPEX, a three-years lifetime for each unit has been set to evaluate a daily CAPEX depreciation. The battery lifetime LT_{batt} has been elaborated from indications available in Ref. [14].

With the adopted parameters, the multi-objective optimization leads to the results reported in Table 3 and plotted in Fig. 5. In particular, Fig. 5 shows the best operation of the three ferries as resulting from the multi-objective D&O optimization. It can be noted that FC tend not to operate at nominal power to avoid higher degradation rates, even though, in some cases, the operation of FC at nominal power could avoid the increase of the battery size. For example, Fig. 5 c shows that the best operation of the medium size ferry requires the FC to work at nominal power for about 4 h in a day. In this way,

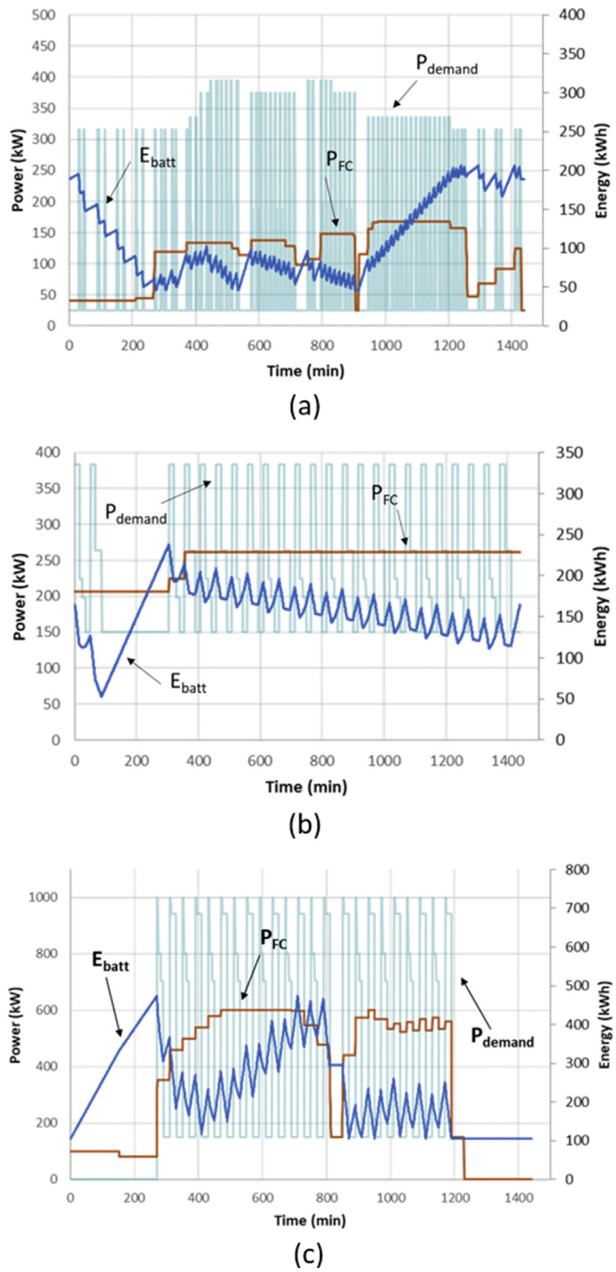

Fig. 5 – Best daily operation of the (a) very small, (b) small, and (c) medium size ferries according to the multi-objective optimization results. For each time step, energy store in the batteries (E_{batt}), FC power output (P_{FC}) and electrical power demand of the ferry (P_{demand}) are represented.

additional CAPEX for FC and battery are avoided, resulting in an overall limitation of the daily cost of the ferry. It is important to note that this aspect is also influenced by the currently high cost of FC and battery (see Table 2), which could rapidly decrease in the next years if such technologies will reach a larger market share, hence modifying the best D&O configuration. However, the proposed optimization model has general validity and can be easily adapted to a wide range of market scenarios (e.g. different CAPEX, overall improvement of units performance, reduced volume and weight of the units, different ship types) by modifying the optimization parameters in Table 2.

To highlight the influence of the FC and battery performance degradation, the multi-objective optimization (MO) results in Table 3 are compared with the ones of a single-objective (SO) optimization reported in Table 4, where only the cost is minimized.

If the minimization of FC degradation is not an optimization criterion, the FC can follow the power demand, possibly with rapid load variation and/or a high number of start/stop cycles. This aspect affects not only the operation, but also the design of the ferry energy systems. As for the operation, it can be seen from the comparison of Table 3 and Table 4 that the FC degradation is significantly higher in SO. In particular, for the very small ferry the FC degradation in SO is about 189% higher than the one in MO. In the considered power profiles and on the basis of the assumptions taken into account, the daily hydrogen consumption remains almost constant. As for the design, the wider range of FC operation to fulfil the power demand in SO results in a lower installed capacity of the batteries (e.g. the battery capacity of the small ferry would be reduced by about 60%). This, in turn, might cause an increase in the overall volume and weight of the shipboard energy conversion and storage units in MO, as it happens for the small size ferry, where volume and weight are increased by about 43% and 41% respectively compared to SO. However, it should be noted that, for all ferries, costs remain almost unchanged from SO case to MO one.

Conclusions

The paper suggests a methodology for the D&O optimization of hybrid PEMFC/Li-ion batteries energy systems for Ro-Pax ferries. Both FC and Li-ion battery performance degradation have been taken into account in the model. More in detail, a MILP approach is adopted to describe conversion and storage energy units and a multi-objective optimization model has been performed for the concurrent minimization of FC degradation and daily CAPEX and OPEX of the vessels. Three ferries are chosen as case studies, to show the ease to adapt the method to different ships, in terms of size, power installed on-board, and daily power demand profile.

The optimization results show that the EMS prevents FC from operating at nominal power to avoid excessive degradation, even if sometimes this operating mode is necessary to limit the overall CAPEX and OPEX cost of the ferry. The multi-objective results were also compared to the ones of a single-objective optimization for the cost minimization, showing that the first approach can potentially reduce FC degradation by up to 65%, without significant changes in costs. The comparison also shows that if FC degradation is minimized, it is necessary to increase the battery capacity by up to 136%, causing an increase in the overall weight and volume of the system, but without exceeding the values of the traditional ICE system currently installed.

Overall, the proposed methodology could be applied for both the preliminary design and the choice of optimal EMS for different size and type of ships, demonstrating the general validity of the method.

Further developments of the model are planned to include detailed modeling of the FC efficiency with load, the Li-ion batteries and the power conditioning system in different operating conditions, and to include heat recovery in the energy system. In addition, solar energy could be considered as an energy input in an improved optimization model.

Declaration of competing interest

The authors declare that they have no known competing financial interests or personal relationships that could have appeared to influence the work reported in this paper.

Acknowledgments

The research has been co-founded by the European Regional Development Fund under the framework of the Regional Operational Program (2014–2020) of the Italian Region Friuli Venezia Giulia (REShiP project). A special thanks to the engineering company Navalprogetti S.r.l. for the support with its experience in the shipping sector, and in particular to Irene Lavagnini for her help in the definition of the case studies.

REFERENCES

[1] Third IMO GHG Study 2014. Executive summary and final report. 2015. Retrieved from, https://safety4sea.com/wp-content/uploads/2015/05/Third-IMO-GHG-Study-Full-Report-5_2015.pdf. [Accessed 26 January 2021].

[2] Reducing emissions from the shipping sector. Retrieved from, https://ec.europa.eu/clima/policies/transport/shipping_en. [Accessed 26 January 2021].

[3] I.M.O. International Maritime Organization. Retrieved from, http://www.imo.org/en/Pages/Default.aspx. [Accessed 26 January 2021].

[4] Tronstad T, Astrand HH, Haugom GP, Langfeldt L. Study on the use of fuel cells in shipping. European Maritime Safety Agency; 2017.

[5] Strategic thinking in sustainable energy, E4tech.. The fuel cell industry review. 2014. Retrieved from, http://www.fuelcellindustryreview.com/archive/TheFuelCellIndustryReview2014.pdf. [Accessed 26 January 2021].

[6] Van Biert L, Godjevac M, Visser K, Aravind PV. A review of fuel cell systems for maritime applications. J Power Sources 2016;327:345–64. https://doi.org/10.1016/j.jpowsour.2016.07.007.

[7] International Maritime Organization, IMO. Draft IGF code agreed. 2014. Retrieved from, http://www.imo.org/en/MediaCentre/PressBriefings/Pages/28-CCC1IGF.aspx#.X4hj7dAzaSk. [Accessed 26 January 2021].

[8] Lloyd GL. Rules for classification and construction, VI.11 guidelines for the use of fuel cell systems on board of ships and boats. 2003. Retrieved from, http://rules.dnvgl.com/docs/

pdf/gl/maritimerules/gl_vi-3-11_e.pdf. [Accessed 26 January 2021].
[9] Vielstich W, Lamm A, Gasteiger H. Handbook of fuel cells: fundamentals technology and applications. Wiley; 2003.
[10] U.S. Department of Energy. Fuel cell handbook. 7th ed. 2004.
[11] European Maritime Safety Agency, EMSA. Study on electrical energy storage for ships. 2020. Retrieved from, http://www.emsa.europa.eu/publications/item/3895-study-on-electrical-energy-storage-for-ships.html. [Accessed 26 January 2021].
[12] SPBES website. Retrieved from, https://spbes.com/. [Accessed 26 January 2021].
[13] Han J, Charpentier JF, Tang T. An energy management system of a fuel cell/battery hybrid boat. Energies 2014;7:2799–820. https://doi.org/10.3390/en7052799.
[14] Pollet BG, Staffell I, Shang JL. Current status of hybrid, battery and fuel cell electric vehicles: from electrochemistry to market prospects. Electrochim Acta 2012;84:235–49. https://doi.org/10.1016/j.electacta.2012.03.172.
[15] Sulaiman N, Hannan MA, Mohamed A, Ker PJ, Majlan EH, Wan Daud WR. Optimization of energy management system for fuel-cell hybrid electric vehicles: issues and recommendations. Appl Energy 2018;228:2061–79. https://doi.org/10.1016/j.apenergy.2018.07.087.
[16] Yue M, Jemei S, Gouriveau R, Zerhouni N. Review on health-conscious energy management strategies for fuel cell hybrid electric vehicles: degradation models and strategies. Int J Hydrogen Energy 2019;44:6844–61. https://doi.org/10.1016/j.ijhydene.2019.01.190.
[17] Geertsma RD, Negenborn RR, Visser K, Hopman JJ. Design and control of hybrid power and propulsion systems for smart ships: a review of developments. Appl Energy 2017;194:30–54. https://doi.org/10.1016/j.apenergy.2017.02.060.
[18] Choi CH, Yu S, Han IS, Kho BK, Kang DG, Lee HY, Seo M, Kong J, Kim G, Ahn J, Park S, Jang D, Lee JH, Kim M. Development and demonstration of PEM fuel-cell-battery hybrid system for propulsion of tourist boat. Int J Hydrogen Energy 2016;41:3591–9. https://doi.org/10.1016/j.ijhydene.2015.12.186.
[19] Taccani R, Malabotti S, Dall'Armi C, Micheli D. High energy density storage of gaseous marine fuels: an innovative concept and its application to a hydrogen powered ferry. Int Shipbuild Prog 2020;1:33–56. https://doi.org/10.3233/ISP-190274.
[20] Rivarolo M, Rattazzi D, Lamberti T, Magistri L. Clean energy production by PEM fuel cells on tourist ships: a time-dependent analysis. Int J Hydrogen Energy 2020;45:25747–57. https://doi.org/10.1016/j.ijhydene.2019.12.086.
[21] Rivarolo M, Rattazzi D, Magistri L. Best operative strategy for energy management of a cruise ship employing different distributed generation technologies. Int J Hydrogen Energy 2018;43:23500–10. https://doi.org/10.1016/j.ijhydene.2018.10.217.
[22] Bassam AM, Phillips AB, Turnock SR, Wilson PA. Development of a multi-scheme energy management strategy for a hybrid fuel cell driven passenger ship. *Int J Hydrogen Energy* 2016;42:623–35. https://doi.org/10.1016/j.ijhydene.2016.08.209.
[23] Bassam AM, Phillips AB, Turnock SR, Wilson PA. An improved energy management strategy for a hybrid fuel cell/battery passenger vessel. Int J Hydrogen Energy 2016;41:22453–64. https://doi.org/10.1016/j.ijhydene.2016.08.049.
[24] Su CL, Wenig XT, Chen CJ. Power generation controls of fuel cell/energy storage hybrid ship power systems. In: IEEE conference and expo transportation electrification asia-pacific (ITEC asia-pacific), Beijing, China; 2014, September. https://doi.org/10.1109/ITEC-AP.2014.6940639.
[25] Wu P, Bucknall R. Hybrid fuel cell and battery propulsion system modelling and multi-objective optimisation for a coastal ferry. Int J Hydrogen Energy 2020;45:3193–208. https://doi.org/10.1016/j.ijhydene.2019.11.152.
[26] Chen H, Pei P, Song M. Lifetime prediction and the economic lifetime of proton exchange membrane fuel cells. Appl Energy 2015;142:154–63. https://doi.org/10.1016/j.apenergy.2014.12.062.
[27] Fletcher T, Thring R, Watkinson M. An Energy Management Strategy to concurrently optimise fuel consumption & PEM fuel cell lifetime in a hybrid vehicle. Int J Hydrogen Energy 2016;41:21503–15. https://doi.org/10.1016/j.ijhydene.2016.08.157.
[28] Balestra L, Schjølberg I. Modelling and simulation of a zero-emission hybrid power plant for a domestic ferry. Int J Hydrogen Energy 2021;46(18):10924–38. https://doi.org/10.1016/j.ijhydene.2020.12.187.
[29] Wang J, Liu P, HIcks-Garner J, Sherman E, Soukiazan S, Verbrugge M, Tataria M, Musser J, Finamore P. Cycle-life model for graphite-LiFePO4 cells. J Power Sources 2011;196:3942–8. https://doi.org/10.1016/j.jpowsour.2010.11.134.
[30] Baghdadi I, Briat O, Delétage JY, Gyan P, Vinassa JM. Lithium battery aging model based on Dakin's degradation approach. J Power Sources 2016;325:273–85. https://doi.org/10.1016/j.jpowsour.2016.06.036.
[31] Schmidt TS, Beuse M, Zhang X, Steffen B, Schneider SF, Pena-Bello A, Bauer C, Parra D. Additional emissions and cost from storing electricity in stationary battery systems. Environ Sci Technol 2019;53:3379–90. https://doi.org/10.1021/acs.est.8b05313.
[32] Terlouw T, AlSkaif T, Bauer C, Van Sark W. Multi-objective optimization of energy arbitrage in community energy storage systems using different battery technologies. Appl Energy 2019;239:356–72. https://doi.org/10.1016/j.apenergy.2019.01.227.
[33] Renkel MF, Lümmen N. Supplying hydrogen vehicles and ferries in Western Norway with locally produced hydrogen from municipal solid waste. Int J Hydrogen Energy 2018;43:2585–600. https://doi.org/10.1016/j.ijhydene.2017.12.115.
[34] Kudria S, Ivanchenko I, Tuchynskyi B, Petrenko K, Karmazin O, Riepkin O. Resource potential for wind-hydrogen power in Ukraine. Int J Hydrogen Energy 2021;46:157–68. https://doi.org/10.1016/j.ijhydene.2020.09.211.
[35] Ramadan M. A review on coupling Green sources to Green storage (G2G): case study on solar-hydrogen coupling. Int J Hydrogen Energy 2021. https://doi.org/10.1016/j.ijhydene.2020.12.165 [in press].
[36] Khelfaoui N, Djafour A, Ghenai C, Laib I, Danoune MB, Gougui A. Experimental investigation of solar hydrogen production PV/PEM electrolyser performance in the Algerian Sahara regions. Int J Hydrogen Energy 2020. https://doi.org/10.1016/j.ijhydene.2020.11.193 [in press].
[37] Gutiérrez-Martín F, Amodio L, Pagano M. Hydrogen production by water electrolysis and off-grid solar PV. Int J Hydrogen Energy 2020. https://doi.org/10.1016/j.ijhydene.2020.09.098 [in press].
[38] Kotowicz J, Jurczyk M, Węcel D. The possibilities of cooperation between a hydrogen generator and a wind farm. Int J Hydrogen Energy 2020. https://doi.org/10.1016/j.ijhydene.2020.11.246 [in press].
[39] Ancona MA, Baldi F, Bianchi M, Branchini L, Melino F, Peretto A, Rosati J. Efficiency improvement on a cruise ship: load allocation optimization. Energy Convers Manag

2018;164:42–58. https://doi.org/10.1016/j.enconman.2018.02.080.
[40] Sakalis GN, Frangopoulos CA. Intertemporal optimization of synthesis, design and operation of integrated energy systems of ships: general method and application on a system with Diesel main engines. Appl Energy 2018;226:991–1008. https://doi.org/10.1016/j.apenergy.2018.06.061.
[41] Dimopoulos GG, Kougioufas AV, Frangopoulos CA. Synthesis, design and operation optimization of a marine energy system. Energy 2008;33:180–8. https://doi.org/10.1016/j.energy.2007.09.004.
[42] Frangopoulos CA. Recent developments and trends in optimization of energy systems. Energy 2018;164:1011–20. https://doi.org/10.1016/j.energy.2018.08.218.
[43] Christidis A, Koch C, Pottel L, Tsatsaronis G. The contribution of heat storage to the profitable operation of combined heat and power plants in liberalized electricity markets. Energy 2012;41:75–82. https://doi.org/10.1016/j.energy.2011.06.048.
[44] Rech S, Lazzaretto A. Smart rules and thermal, electric and hydro storages for the optimum operation of a renewable energy system. Energy 2018;147:742–56. https://doi.org/10.1016/j.energy.2018.01.079.
[45] Baldi F, Ahlgren F, Melino F, Gabrielii C, Andersson K. Optimal load allocation of complex ship power plants. Energy Convers Manag 2016;124:344–56. https://doi.org/10.1016/j.enconman.2016.07.009.
[46] Ito K, Yokoyama R, Shiba T. Optimal operation of a diesel engine cogeneration plant including a heat storage tank. J Eng Gas Turbines Power 1992;114:687–94. https://doi.org/10.1115/1.2906643.
[47] Rech S. Smart energy systems: guidelines for modelling and optimizing a fleet of units of different configurations. Energies 2019;12:1320. https://doi.org/10.3390/en12071320.
[48] MarineTraffic Global. Ship tracking intelligence. Retrieved from, https://www.marinetraffic.com/. [Accessed 19 April 2020].
[49] Wang S, Meng Q. Sailing speed optimization for container ships in a liner shipping network. Transport Res Part E 2012;48:701–14. https://doi.org/10.1016/j.tre.2011.12.003.
[50] Klebanoff LE, Pratt JW, Madsen RT, Caughlan SAM, Leach TS, Appelgate TB, Kelety SZ, Wintervoll H, Haugom GP, Teo ATY. The zero-V: feasibility of a liquid hydrogen fueled coastal research vessel. Retrieved from, https://glosten.com/wp-content/uploads/2018/07/SAND2018-4664_Zero-V_Feasibility_Report_8.5x11_Spreads_FINALDRAFT_compress.pdf. [Accessed 5 June 2020].
[51] NCE Maritime CleanTech. Norwegian future value chains for liquid hydrogen. 2019. Retrieved from, https://maritimecleantech.no/wp-content/uploads/2016/11/Report-liquid-hydrogen.pdf. [Accessed 28 August 2020].
[52] Madsen RT, Klebanoff LE, Caughlan SAM, Pratt JW, Leach TS, Appelgate TB, Kelety SZ, Wintervoll HC, Haugom GP, Teo ATY, Ghosh S. Feasibility of the Zero-V: a zero-emissions hydrogen fuel-cell coastal research vessel. Int J Hydrogen Energy 2020;45:25328–43. https://doi.org/10.1016/j.ijhydene.2020.06.019.
[53] Klebanoff LE, Pratt JW, LaFleur CB. Comparison of the safety-related physical and combustion properties of liquid hydrogen and liquid natural gas in the context of the SF-BREEZE high-speed fuel-cell ferry. Int J Hydrogen Energy 2017;42:757–74. https://doi.org/10.1016/j.ijhydene.2016.11.024.
[54] Jeong J, Seo S, You H, Chang D. Comparative analysis of a hybrid propulsion using LNG-LH2 complying with regulations on emissions. Int J Hydrogen Energy 2018;43:3809–21. https://doi.org/10.1016/j.ijhydene.2018.01.041.
[55] Aarskog FG, Hansen OR, Strømgren T, Ulleberg O. Concept risk assessment of a hydrogen driven high speed passenger ferry. Int J Hydrogen Energy 2020;45:1359–72. https://doi.org/10.1016/j.ijhydene.2019.05.128.
[56] Python website. Retrieved from, https://www.python.org/. [Accessed 4 September 2020].
[57] Gurobi optimizer website. Retrieved from, https://www.gurobi.com/. [Accessed 4 September 2020].
[58] Hydrogenics website. Retrieved from, https://www.hydrogenics.com/. [Accessed 4 September 2020].
[59] Powercell website. Retrieved from, https://www.powercell.se/en/start/. [Accessed 4 September 2020].
[60] Proton-Motor website. Retrieved from, https://www.proton-motor.de/. [Accessed 4 September 2020].
[61] Nedstack website. Retrieved from, https://nedstack.com/en. [Accessed 4 September 2020].
[62] Linde website. Retrieved from, https://www.linde-engineering.com/en/images/P_3_3_e_12_150dpi_tcm19-5774.pdf. [Accessed 4 September 2020].
[63] Air liquide website. Retrieved from, https://airliquide-expertisecenter.com/cryogenic-gases/. [Accessed 4 September 2020].
[64] Praxair website. Retrieved from, https://www.praxairusa.com/gas-supply-modes/microbulk-tanks. [Accessed 4 September 2020].